Journal of Alloys and Compounds 515 (2012) 86–89

Contents lists available at SciVerse ScienceDirect

Journal of Alloys and Compounds

journal homepage: www.elsevier.com/locate/jallcom

Solid-state phase transformation-induced heterogeneous duplex structure in Ti–Sn–Fe alloys

E.M. Park[a], G.A. Song[a], J.H. Han[a], Y. Seo[b], J.Y. Park[a], K.B. Kim[a,*]

[a] HMC & INAME, Faculty of Nanotechnology and Advanced Materials Engineering, Sejong University, 98 Gunja-dong, Gwnagjin-gu, Seoul 143-747, Republic of Korea
[b] GRI & HMC, Faculty of Nanotechnology and Advanced Materials Engineering, Sejong University, Gunja-dong, Gwangjin-gu, Seoul 143-747, Republic of Korea

ARTICLE INFO

Article history:
Received 16 August 2011
Received in revised form 8 November 2011
Accepted 17 November 2011
Available online 9 December 2011

Keywords:
Nanostructured materials
Rapid-solidification
Mechanical properties
Scanning electron microscopy

ABSTRACT

Systematic microstructural investigations reveal that heterogeneous duplex structure in Ti–Sn and Ti–Sn–Fe alloys consisting of an array of Ti_3Sn plates surrounding the duplex colony and ultrafine twin results from solid-state decomposition of supersaturated β-Ti into α-Ti + Ti_3Sn phases. Moreover, small addition of Fe into the $Ti_{82}Sn_{18}$ duplex alloy has a strong influence to refine the twinning in the Ti_3Sn phase and interlayer spacing of the duplex structure. Such microstructural heterogeneities are effective to enhance both strength and plasticity at room temperature. Based on these results, it is possible to design the unique ultrafine duplex structure with high strength and large plasticity together by introducing the solid-state phase transformation-induced heterogeneity.

1. Introduction

Development of ultrafine eutectic composites consisting of micron-scale dendrites and nano-/ultrafine eutectic matrix has been highlighted as one of ways to achieve high strength alloys combined with large plasticity at room temperature [1,2]. Further detailed investigations on the deformation mechanisms of such ultrafine eutectic composites have pointed out that the strength and plasticity of the samples are strongly depending on the slip deformation in the micron-scale dendrites and shear deformation in the ultrafine eutectic matrix, respectively [3–7]. Along the line to optimize the mechanical properties based on the modulation of the microstructure, a series of simple ultrafine eutectic alloys even without the micron-scale dendrites can also exhibit macroscopic plastic strain by formation of the spherical morphology of the eutectic colonies effective to dissipate the localized stress through a rotation of the spherical eutectic colonies [8]. Hence, it is believed that the strength and plasticity of the ultrafine eutectic alloys can be optimized by controlling the structural heterogeneities including volume fraction, length-scale and morphology of the microstructure.

Besides the structural heterogeneities in the ultrafine eutectic alloys, there are several trials to introduce the chemical heterogeneities in the ultrafine eutectic alloys so called bimodal eutectic structure, i.e. a mixture of two eutectic structures with the different constituent phases at each eutectic entity [9–12]. For example, the bimodal eutectic composites in a series of $(Ti_{70.5}Fe_{29.5})_{100-x}Sn_x$ alloys with $x = 5$, 7 and 9 consisting of a mixture of micron-scale Ti_3Sn dendrite phase, and coarse (β-Ti + Ti_3Sn) and fine eutectic (β-Ti + TiFe) in matrix can also present a good combination of a strength of ~1.3 GPa and plasticity of ~15.7% [9]. The formation mechanisms of such bimodal eutectic structure containing the chemical heterogeneities can be originated by quasi-peritectic reaction cooperated with two distinct univariant reactions upon solidification [13]. Furthermore, the asymmetrical solubility and immiscibility of the minor elements in the ultrafine eutectic alloys can be treated as one of the chemical heterogeneities to control the mechanical properties of the ultrafine eutectic alloys.

Indeed, both structural and chemical heterogeneities play an important role to dissipate the localization of the stress thus enhancing the macroscopic plasticity of the ultrafine eutectic alloys. However, one can find that the enhancement of the plasticity by introducing either structural or chemical heterogeneities in the ultrafine eutectic alloys often comes along the decrease of the strength of the samples. This implies that the well-known strength–plasticity relationship obtained from conventional alloys can be applicable to such ultrafine eutectic alloys and composites. Therefore, it is necessary to find out the ways to design the microstructure of the ultrafine eutectic alloys to enhance the plasticity without deteriorating the strength.

2. Experimental

A series of $(Ti_{82}Sn_{18})_{100-x}Fe_x$ alloys with $x = 0$, 1 and 3 at.% were prepared by arc melting of the pure elements under argon atmosphere and directly

* Corresponding author. Tel.: +82 2 3408 3690; fax: +82 2 3408 3664.
E-mail addresses: kbkim@sejong.ac.kr, kibuem@googlemail.com (K.B. Kim).

0925-8388/$ – see front matter © 2011 Elsevier B.V. All rights reserved.
doi:10.1016/j.jallcom.2011.11.078

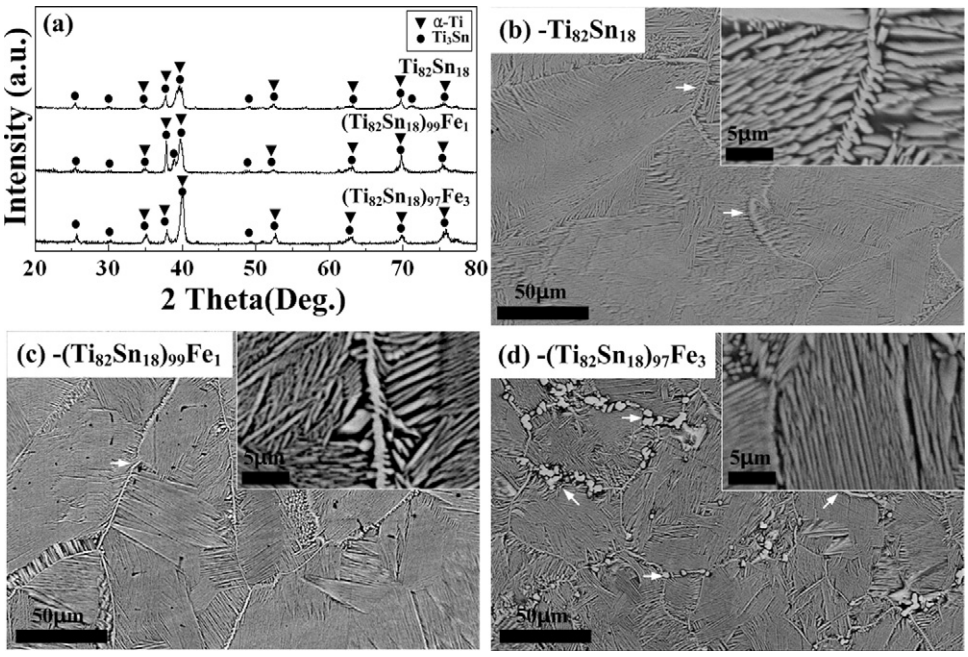

Fig. 1. XRD patterns (a) and backscattered electron SEM micrographs [(b)–(d)] of the $(Ti_{82}Sn_{18})_{100-x}Fe_x$ alloys ($x = 0$, 1 and 3).

casted into cylindrical rods shape with 3 mm diameter and 50 mm length using a in situ suction casting facility. The microstructures of as-cast sample were examined using scanning electron microscopy (SEM) (JEOL, JSM-6390). X-ray diffraction (XRD) (Rigaku RINT2000, monochromatic Cu Kα radiation) was employed for the phase identification. Transmission electron microscopy (TEM: JEM 2010) was used for a structural characterization. Thin foils for TEM were prepared by conventional ion milling (Gatan, Model 600). The room temperature mechanical properties were evaluated by uniaxial compression tests with 2:1 aspect ratio cylindrical specimens under loading at an initial strain rate of $1 \times 10^{-3}\ s^{-1}$.

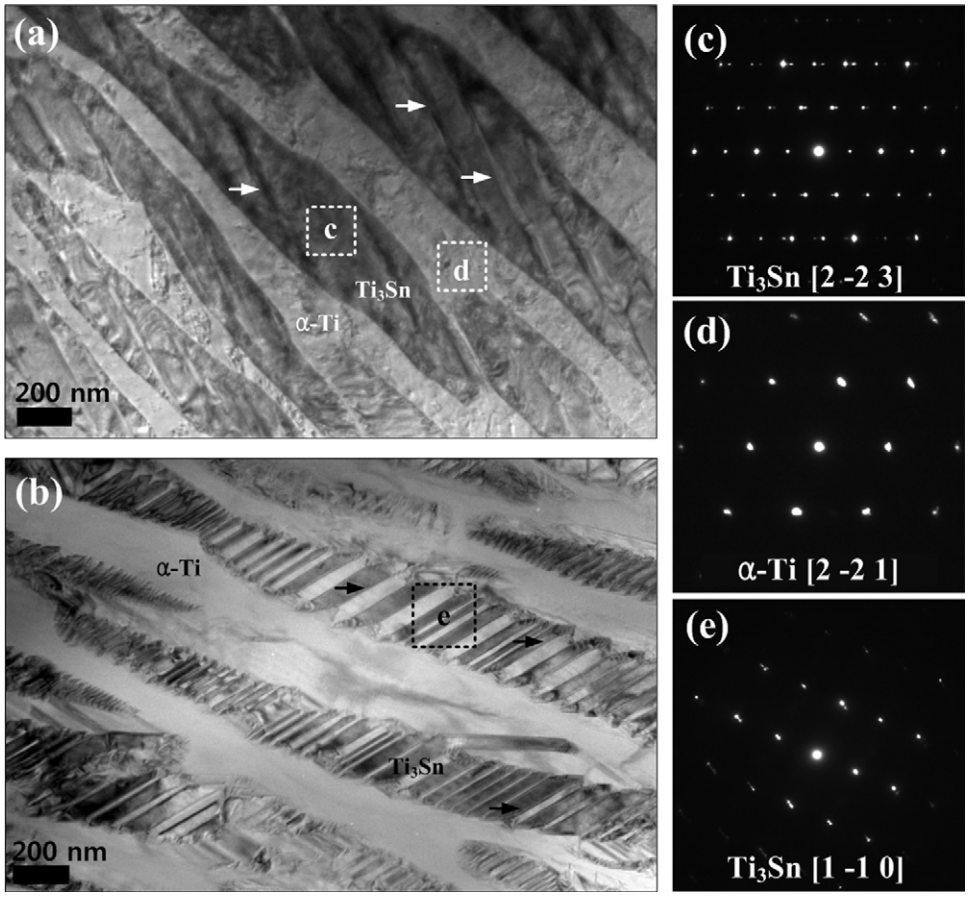

Fig. 2. Bright field TEM images of the $Ti_{82}Sn_{18}$ (a) and $(Ti_{82}Sn_{18})_{97}Fe_3$ (b) and corresponding selected area diffraction patterns [(c)–(e)].

3. Results and discussions

Fig. 1 shows XRD patterns (a) and backscattered electron (BSE) micrographs [(b)–(d)] of as-cast $(Ti_{82}Sn_{18})_{100-x}Fe_x$ alloys with $x = 0$, 1 and 3. The main sharp XRD diffraction peaks in Fig. 1(a) can be identified as a mixture of hexagonal α-Ti ($P6_3/mmc$) solid solution and hexagonal Ti_3Sn ($P6_3/mmc$) intermetallic compound. Moreover, there is no significant change on the diffraction peaks with increasing Fe content implying that the minor addition of Fe has no strong effect on the phase formation upon solidification.

The BSE image of a binary $Ti_{82}Sn_{18}$ duplex alloy shown in Fig. 1(b) displays typical lamellar-type duplex structure with an interlayer spacing of 800–1000 nm. Moreover, the size of the ultrafine duplex colony encapsulated by the phase with bright contrast as indicated by arrows can be measured to be 100–170 μm throughout the sample. By combining XRD and SEM results, the bright and dark phases can be identified as Ti_3Sn and α-Ti phases, respectively. Similarly, the microstructure of as-cast $(Ti_{82}Sn_{18})_{99}Fe_1$ alloy shown in Fig. 1(c) is more and less identical to that of the as-cast $Ti_{82}Sn_{18}$ alloy in Fig. 1(b). However, one can find the decrease of the lamellar spacing, i.e. 450–900 nm and size of the ultrafine duplex colony, i.e. 80–130 μm. With further increasing Fe content, i.e. $(Ti_{82}Sn_{18})_{97}Fe_3$ alloy shown in Fig. 1(d), it is clearly visible to further refinement of the duplex colony down to 40–80 μm. Accordingly, there is a significant increase of the volume fraction of the Ti_3Sn phase along the grain boundary as indicated by arrows in Fig. 1(d). Furthermore, the morphology of the duplex colony is rather spherical. Hence, it is possible to conclude that the addition of Fe into the $Ti_{82}Sn_{18}$ duplex alloy has a strong effect to decrease the size of the duplex colony and to increase the volume fraction of the Ti_3Sn phase surrounding the colony accompanying the spheroidization of the duplex colony.

In general, it is well known that the typical duplex structure, such as laminated structure, forms by eutectic reaction [14]. However, the microstructure of the Ti–Sn(–Fe) alloys is quite distinctive, i.e. Ti_3Sn phase encapsulating the colony and the morphology of duplex structure as shown in Fig. 1, compared with other typical eutectic alloys [15]. These microstructural characteristics point out that the lamellar structure does not originate from the Ti–Sn binary eutectic reaction. Moreover, the constitutive phases of the entire alloys are identified as a mixture of α-Ti solid solution and Ti_3Sn intermetallic compound, indicating that complete solid phase transformation takes place, such as β-Ti to α-Ti, based on the Ti–Sn binary phase diagram [16]. It has been reported that FeCo-based multi-component alloys consist of primary dendrite comprising duplex-type morphology, which results from precipitation during solidification [17]. In the present investigation, the cast samples have been prepared by a direct Cu mold casting into cylindrical rods with 3 mm diameter and 50 mm length using a suction casting facility in order to guarantee a high cooling rate to obtain the ultrafine microstructure. Therefore, it is believed that this high cooling rate could result in a minute shift of eutectic point ($Ti_{82}Sn_{18}$) into the Ti_3Sn phase field in the Ti-rich corner of Ti–Sn binary phase diagram, which leads to the formation of primary β-Ti phases supersaturated in Sn throughout the samples. As the temperature decreases from 1873 K to 1184 K, Sn content in primary β-Ti phase moves mainly toward boundary regions and Ti_3Sn phase are precipitated as a form of the array of plates shown in Fig. 1 [(b)–(d)]. Once the temperature passes 1184 K, the eutectoid reaction of β-Ti into α-Ti + Ti_3Sn takes place, which causes the formation of the duplex structure shown in Fig. 1. Hence, it is possible to suggest that the unique duplex structure can be formed by the solid-state phase transformation.

Fig. 2 shows bright field TEM images of the $Ti_{82}Sn_{18}$ (a) and $(Ti_{82}Sn_{18})_{97}Fe_3$ (b) alloys and corresponding selected area diffraction patterns [(c)–(e)]. Fig. 2(a) shows the bright-field image

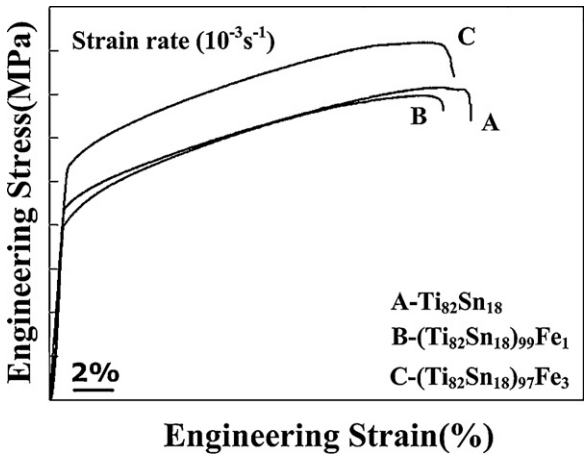

Fig. 3. Stress–strain curves of the Ti–Sn–Fe alloys at room temperature compression: (a) $Ti_{82}Sn_{18}$, (b) $(Ti_{82}Sn_{18})_{99}Fe_1$, and (c) $(Ti_{82}Sn_{18})_{97}Fe_3$ alloy.

obtained from duplex structure in Fig. 1(b). The interlayer spacing is measured to be of order of 800–850 nm, which is good agreement with the SEM analysis in Fig. 1(b). Interestingly, one can observe that typical line contrast often obtaining from typical twinning is homogeneous distributed inside the dark contrast areas as denoted by arrows in Fig. 2(a). Furthermore, the spacing of the line contrast can be measured to be about 160–300 nm. The selected area diffraction patterns in Figs. 2[(c) and (d)] obtained from the dark and bright contrast areas denoted as 'c' and 'd' in Fig. 2(a) correspond to the [2–23] and [2–21] zone axes of the hexagonal Ti_3Sn and α-Ti phases, respectively. Moreover, it is worth to note that the splitting diffraction intensity from the Ti_3Sn phase as shown in Fig. 2(c) is clearly visible indicating the formation of twinning in the Ti_3Sn phase. Fig. 2(b) presents bright-field TEM image of $(Ti_{82}Sn_{18})_{97}Fe_3$ alloy, which has analogous lamellar structure of dark and bright areas to that of $Ti_{82}Sn_{18}$ binary alloy in Fig. 2(a). Fig. 2(e) shows the SADP from the Ti_3Sn phase at zone axis of [1–10], indicating formation of twins on Ti_3Sn phase, similar to binary Ti–Sn alloys in Fig. 2(c). Moreover, it is clearly observed that spacing of the twin formed on the Ti_3Sn phase considerably decreases down to 40–50 nm in comparison with Fig. 2(a), suggesting that Fe content serves a vital function in refine the twinning in the Ti_3Sn phase.

Fig. 3 shows typical stress–strain curves of the $(Ti_{82}Sn_{18})_{100-x}Fe_x$ ($x = 0$, 1 and 3) alloys under room temperature compression. The binary $Ti_{82}Sn_{18}$ alloy possesses the yield strength of ~780 MPa and ultimate fracture strength of 1394 MPa with a plasticity of ~21%. The yield and ultimate fracture strength of the Ti–Sn–Fe alloys gradually increases up to 1045 MPa and 1635 MPa, respectively, with further increase in Fe (1, 3 at.%) content while the good plasticity is retained (21–23%).

It has been reported that microstructural heterogeneities are effective to improve the mechanical properties of the ultrafine eutectic alloys [9]. Several trials to introduce heterogeneities into microstructure of ultrafine eutectic alloys have been made. Recent investigations point out that structural, i.e. length-scale and morphology, and chemical, i.e. constituent phases, heterogeneities can be achieved by modification of eutectic colony morphology and quasi-peritectic reaction [13]. In the present study, the unique duplex structure containing microstructural heterogeneity, i.e. the Ti_3Sn phase encapsulating the colony and ultrafine twinning, is formed by solid-state phase transformation, which is possibly responsible for enhancement of the mechanical properties of the Ti–Sn–Fe duplex alloys.

In general, the mechanical properties of the ultra-fine composites having alternating lamellar layers can be governed by the length-scale and volume fraction of the micron-scale primary phase

and ultra-fine matrix [4–8]. For example, a decrease in the lamellar spacing of the eutectic matrix in Ti-based ultra-fine eutectic composites results in the enhancement of the strength [3–18]. In this scenario, systematic microstructural investigation reveals the Fe addition into the binary Ti–Sn alloy can have a strong influence to reduce the lamellar spacing and further refine twinning in Ti_3Sn phase, which is a key to increasing the strength of the Ti–Sn–Fe alloys. In addition, entire Ti–Sn–Fe duplex alloys contain the Ti_3Sn phase surrounding the α-Ti + Ti_3Sn duplex structure as shown in Fig. 1. This can be characterized as one of structural heterogeneities which is effective not only in suppressing propagation of shear hands but also in dissipating shear stress, and thus plays an important role in the improvement of the plasticity of the Ti–Sn–Fe alloys. Therefore, it is suggested that the unique heterogeneous duplex structure induced by the solid-state phase transformation is effective in enhancing both strength and plasticity.

4. Summary

A series of $(Ti_{82}Sn_{18})_{100-x}Fe_x$ alloys with $x = 0$, 1 and 3 has been successfully prepared by using suction casting. Systematic investigation of the microstructure reveals that the unique heterogeneous duplex structure containing an array of Ti_3Sn plates encapsulating the duplex colony and ultrafine twin originates from solid-state transformation and the addition of Fe into binary $Ti_{82}Sn_{18}$ alloy induces a reduction in the interlayer spacing and the refinement of the twinning. The microstructural heterogeneities in the duplex alloys play a vital role in improving both strength and plasticity.

Acknowledgements

This work was supported by the Global Research Laboratory (GRL) Program and the National Research Foundation of Korea (NRF) grant funded by the Korea government (MEST) of Korea Ministry of Education, Science and Technology (No. 2010–0013854). One of the authors, Y. Seo, specially thanks to the support from Priority Research Centers Program through the National Research Foundation of Korea (NRF) funded by the Ministry of Education, Science and Technology (2010-0020207).

References

[1] G. He, J. Eckert, W. Loser, L. Schultz, Nat. Mater. 2 (2003) 33–37.
[2] E. Ma, Nat. Mater. 2 (2003) 7–8.
[3] J.M. Park, K.B. Kim, W.T. Kim, M.H. Lee, J. Eckert, D.H. Kim, Intermetallics 16 (2008) 642–650.
[4] K.B. Kim, J. Das, W. Xu, Z.F. Zhang, J. Eckert, Acta Mater. 54 (2006) 3701–3711.
[5] D.V. Louzguine, L.V. Louzguina, H. Kato, A. Inoue, Acta Mater. 53 (2005) 2009–2017.
[6] J. Das, K.B. Kim, F. Baier, W. Löser, J. Eckert, J. Appl. Phys. Lett. 87 (2005) 161907.
[7] K.B. Kim, J. Das, F. Baier, J. Eckert, J. Alloys Compd. 434–435 (2007) 106–109.
[8] J.M. Park, K.B. Kim, W.T. Kim, D.H. Kim, Appl. Phys. Lett. 91 (2007) 131907.
[9] J.H. Han, K.B. Kim, S. Yi, J.M. Park, S.W. Sohn, T.E. Kim, D.H. Kim, J. Das, J. Eckert, Appl. Phys. Lett. 93 (2008) 141901.
[10] G.A. Song, W.H. Lee, N.S. Lee, J.M. Park, D.H. Kim, D.H. Kim, J.S. Lee, J.S. Park, K.B. Kim, J. Mater. Res. 24 (2009) 2892–2898.
[11] J.H. Han, K.B. Kim, S. Yi, J.M. Park, D.H. Kim, S. Pauly, J. Eckert, Appl. Phys. Lett. 93 (2008) 201906.
[12] J.M. Park, N. Mattern, U. Kühn, J. Eckert, K.B. Kim, W.T. Kim, K. Chattopadhyay, D.H. Kim, J. Mater. Res. 24 (2009) 2605–2609.
[13] G.A. Song, J.H. Han, T.E. Kim, J.M. Park, D.H. Kim, S. Yi, Y. Seo, N.S. Lee, K.B. Kim, Intermetallics 19 (2011) 536–540.
[14] J. Lindemann, L. Wagner, Mater. Sci. Eng. A: Struct. 263 (1999) 137–141.
[15] D.V. Louzguine, H. Kato, L.V. Louzguina, A. Inoue, J. Mater. Res. 19 (2004) 3600–3606.
[16] T.B. Massalski, Binary Alloy Phase Diagram, ASM International, West Cohshohocken, PA, 1990.
[17] R. Li, G. Liu, M. Stoica, J. Eckert, Intermetallics 18 (2010) 134–139.
[18] J.M. Park, S. Pauly, N. Mattern, D.H. Kim, K.B. Kim, J. Eckert, Adv. Eng. Mater. 12 (2010) 1137–1141.